Delicate semimetals: Protected gapless phases from unstable homotopies

Bhandaru Phani Parasar* and Vijay B. Shenoy†
Centre for Condensed Matter Theory, Department of Physics, Indian Institute of Science, Bangalore 560012, India

(Received 27 September 2023; accepted 13 March 2024; published 10 April 2024)

We construct and explore two-band topological semimetals in different spatial dimensions that are protected by unstable homotopies. Dubbed "delicate semimetals," they generically host nodal lines and are inspired by the example of such phases realized in four dimensions arising from maps from the three-torus T^3 [Brillouin zone of a three-dimensional (3D) crystal] to the two-sphere S^2 related to the Hopf map. In the four-dimensional example, a surface enclosing such a nodal line in the Brillouin zone carries a Hopf flux. These four-dimensional semimetals show a unique class of surface states: while some 3D surfaces host gapless Fermi-arc states *and* drumhead states, other surfaces have gapless Fermi surfaces. Gapless two-dimensional corner states are also present at the intersection of three-dimensional surfaces. We also demonstrate such semimetals realized in three dimensions in chiral class AIII, which arise from the unstable homotopies of maps from T^2 (Brillouin zone of a two-dimensional crystal) to S^1. These 3D semimetals also host nodal lines, accompanied by a rich collection of surface states, including drumhead type. This work provides a new framework to realize protected nodal line semimetals, particularly in synthetic quantum systems such as cold atoms, photonic, and topoelectric systems.

DOI: 10.1103/PhysRevB.109.155131

I. INTRODUCTION

The understanding and classification of gapped topological phases [1–8] of noninteracting fermions has not only provided deeper insights, but also, stimulated wider generalizations [9,10] and the search for topological materials [11]. The current understanding of these gapped phases is built on the symmetry classification of the fermionic systems that arise from the presence or absence of intrinsic symmetries such as time reversal, charge conjugation and sublattice symmetries [8,12–14]. In a crystalline system in d dimensions, the ground state of a gapped fermionic system is obtained by the state of occupied valence bands in the first Brillouin zone (BZ), the d-torus T^d. Interestingly, the occupied states at any point in the BZ can be viewed as a point in one of the ten symmetric spaces $\mathcal{S}$, the specific one being determined by the intrinsic symmetry. Topologically distinct gapped ground states are identified with the homotopy classes of maps from T^d to $\mathcal{S}$, resulting in the periodic table of strong topological phases [5].

Apart from these symmetry-protected topological phases, a class of gapless phases has elicited attention, beginning with graphene [15], and, more recently, Weyl and Dirac semimetals [16–22]. Weyl semimetals arise in three dimensions, exploiting the topology in a lower-dimensional slice of the Brillouin zone (say the k_1-k_2 plane) that undergoes a "phase transition" as the k_3 of the slice is varied. Thus, these semimetals are protected by the topology of the two adjacent two-dimensional phases, the gapless points being those k_3 at which the quantum phase transition between the two-dimensional phases is affected. They have received considerable attention owing to their exotic properties such as Fermi-arc surface states and interesting nonlinear responses related to the chiral anomaly. A key question to be explored is a general classification of such semimetallic phases including the role of lattice symmetries.

In this context, it is useful to recall that the classification of gapped phases hinges on the number of bands being large. In more mathematical terms, these are determined by the *stable homotopies* of maps from T^d to $\mathcal{S}$ which are realized when $\mathcal{S}$ is large dimensional. In the absence of a large number of bands, one can still obtain topological phases that arise from unstable homotopies [23] of maps from T^d to $\mathcal{S}$ i.e., when the space $\mathcal{S}$ is "small dimensional" [24]. An example in a three-dimensional lattice that hosts a two-band gapped system is dubbed as a "Hopf insulator"[25–28] whose topology can be traced to the homotopies of maps from the three-sphere S^3 to the two-sphere S^2; this has recently been realized in a topoelectrical system [29]. In relation to more recent work on topological systems beyond the stable classification, further classifying gapped phases as "fragile" [30], or "delicate"[31,32], Hopf insulators fall in the delicate class. These ideas lead to an interesting question in the context of semimetals—are there semimetals that are protected by unstable homotopies?

In this paper, we answer this question in the affirmative by constructing examples of semimetals protected by unstable homotopies in different dimensions. Our primary example shows how a Hopf insulator in three dimensions can be used to construct interesting gapless phases in four dimensions with several new features. Unlike the Weyl semimetal in three dimensions, these four-dimensional (4D) semimetals host nodal lines of gapless points (a one-dimensional submanifold) in the four-dimensional Brillouin zone. Remarkably, any three-dimensional (3D) surface that encloses one of these rings carries an integer Hopf number that characterizes the

*bhandarup@iisc.ac.in
†shenoy@iisc.ac.in

 ©2024 American Physical Society

phases on either side of these rings. These features manifest spectacularly in the nature of gapless surface states. There are three-dimensional surfaces, which host Fermi-arc states and, in addition, gapless drumhead states [33]. Furthermore, we also find evidence of two-dimensional corner states that arise at the intersection of two three-dimensional surfaces of the four-dimensional insulator. As a second example, we construct two-band gapless phases in three spatial dimensions in symmetry class AIII (the chiral class) that host nodal lines, and gapless surface states, including drumhead variety. These three-dimensional semimetals are protected by the unstable homotopies of maps from T^2 (BZ of two-dimensional crystal) to S^1. This work thus presents a new class of gapless phases—dubbed "delicate semimetals"—inspired by the four-dimensional example constructed from the Hopf insulator with delicate topology [31,32,34] that are protected by unstable homotopies. This work contributes to the problem of classification of gapless phases and also provides routes to realizing interesting topological gapless phases in higher dimensions [35–37].

In the next section (Sec. II) we review Hopf and Hopf-Chern insulators. This is followed by Sec. III which constructs 4D semimetallic phases arising from Hopf insulators. Section IV constructs a 3D example with AIII symmetry. The paper concludes in Sec. V with a brief discussion on perspectives.

II. HOPF AND HOPF-CHERN INSULATORS

We begin with a two-band system that realizes an insulting phase on a 3D cubic lattice with a unit lattice spacing. The Brillouin zone (BZ) of this system is the three torus T^3 corresponding to $[-\pi, \pi]^3$. A generic point in the BZ is denoted by $\boldsymbol{k} = (k_1, k_2, k_3)$. A two-band Hamiltonian is defined by

$$H(\boldsymbol{k}) = \boldsymbol{d}(\boldsymbol{k}) \cdot \boldsymbol{\sigma}, \tag{1}$$

where $\boldsymbol{d}(\boldsymbol{k})$ is the vector $(d_1(\boldsymbol{k}), d_2(\boldsymbol{k}), d_3(\boldsymbol{k}))$, and $\boldsymbol{\sigma} = (\sigma_1, \sigma_2, \sigma_3)$ where σ_i are the 2×2 Pauli matrices. The chemical potential here and henceforth in this paper is set to zero so that the fermionic many-body system is half filled (1 particle per site). Existence of a gap necessitates that $|\boldsymbol{d}(\boldsymbol{k})| > 0$ for $\boldsymbol{k} \in T^3$, and thus the unit vector $\hat{d}(\boldsymbol{k}) = \boldsymbol{d}(\boldsymbol{k})/|\boldsymbol{d}(\boldsymbol{k})|$ can be identified with a point on the two-sphere S^2. Consequently, the Hamiltonian (1) can be viewed as a map from T^3 to S^2.

Distinct insulating topological phases are obtained depending on the homotopy class of the map from T^3 to S^2, with two insulators being identical if they can be smoothly deformed to each other (i.e., homotopic) without closing the gap. Such maps have been extensively studied both from the mathematical and physical perspectives [38–42]. The homotopy classes of the maps are characterized by four (integer) numbers $(\chi, (C_1, C_2, C_3))$. The numbers C_α are the Chern numbers associated with two-dimensional T^2 submanifolds of T^3, where α indicates the normal direction to the T^2-submanifold. The number χ is in $\mathbb{Z}_{2Q}$ where $Q = \mathrm{GCD}(C_1, C_2, C_3)$. Thus, if all C_α are zero, χ can take any integer value, and such insulators are termed as Hopf insulators [25–27]. On the other hand, if any of the C_α is nonzero, then χ takes on only a finite set of values, and such insulators are dubbed as Hopf-Chern insulators [27].

Hopf insulators can be constructed [25,26] using an intermediate map from T^3 to S^3 (the three-sphere). Since S^3 is described by two complex numbers z_1, z_2 such that $|z_1|^2 + |z_2|^2 > 0$, the prescription

$$\begin{aligned} z_1(\boldsymbol{k}, h) &= \sin k_1 + \mathbb{i} \sin k_2, \\ z_2(\boldsymbol{k}, h) &= \sin k_3 + \mathbb{i}(\cos k_1 + \cos k_2 + \cos k_3 + h) \end{aligned} \tag{2}$$

(h is a parameter, $\mathbb{i} = \sqrt{-1}$), is a map from T^3 to S^3. The topological index Γ (Sec. S1 of the Supplemental Material [43]) of this map vanishes when $|h| > 3$, is 1 for $1 < |h| < 3$, and -2 for $|h| < 1$. The map is thus topologically nontrivial for $|h| < 3$. Finally, to obtain a two-band model, the point on S^3 is mapped to S^2 via the Hopf map [44]

$$\begin{aligned} \boldsymbol{d}^{(p,q)}(\boldsymbol{k}, h) = \big(&2\mathrm{Re}\big[z_1^p(\boldsymbol{k}, h) z_2^{*q}(\boldsymbol{k}, h)\big], \\ &2\mathrm{Im}\big[z_1^p(\boldsymbol{k}, h) z_2^{*q}(\boldsymbol{k}, h)\big], \\ &|z_1(\boldsymbol{k}, h)|^{2p} - |z_2(\boldsymbol{k}, h)|^{2q}\big), \end{aligned} \tag{3}$$

where p, q are coprime integers, and $*$ denotes complex conjugation. Such a map has a Hopf index [44] $\mathscr{H} = \pm pq$. The Hopf insulator defined using Eq. (3) has vanishing Chern number C_α, and is thus characterized by $(\chi, (0, 0, 0))$ where $\chi = \Gamma \mathscr{H}$ [26]. The invariant χ can be written as [45]

$$\chi = -\int_{\mathrm{BZ}} d^3\boldsymbol{k}\, A_\mu(\boldsymbol{k}) F_\mu(\boldsymbol{k}), \tag{4}$$

where μ runs over 1,2,3 (summation convention implied)

$$F_\mu(\boldsymbol{k}) = \frac{1}{8\pi} \epsilon_{\mu\nu\sigma} \epsilon_{abc} \hat{d}^a(\boldsymbol{k}) \partial_{k_\nu} \hat{d}^b(\boldsymbol{k}) \partial_{k_\sigma} \hat{d}^c(\boldsymbol{k}), \tag{5}$$

where latin letters a, b, c run over 1,2,3). Also, $F_\mu(\boldsymbol{k}) = \epsilon_{\mu\nu\sigma} \partial_{k_\mu} A_\sigma(\boldsymbol{k})$.

Hopf-Chern insulators are those which have nonzero Chern numbers C_α. These are obtained [27,32,34,46] (see also Ref. [47] for Hopf-Chern systems apropos flat-band physics) using

$$\begin{aligned} \begin{pmatrix} d_1^{(m)}(\boldsymbol{k}) \\ d_2^{(m)}(\boldsymbol{k}) \end{pmatrix} &= \begin{pmatrix} \cos mk_1 & -\sin mk_1 \\ \sin mk_1 & \cos mk_1 \end{pmatrix} \begin{pmatrix} \sin k_2 \\ \sin k_3 \end{pmatrix}, \\ d_3^{(m)}(\boldsymbol{k}) &= 1 + \Delta_1(\cos k_2 + \cos k_3) + \Delta_2 \cos k_2 \cos k_3, \end{aligned} \tag{6}$$

where m is an integer and Δ_1, Δ_2 are real parameters. For this model, $C_2 = C_3 = 0$ always, and C_1 is determined by the values of Δ_1 and Δ_2 (and is not affected by the value of m). The quantity χ is determined by m as $\chi = m|C_1| \bmod 2|C_1|$.

III. FOUR-DIMENSIONAL SEMIMETALS

Realization of such topological phases in d dimensions allows us to construct interesting semimetallic phases in $d + 1$ dimensions. In fact, the well-studied Weyl semimetallic phases are examples of such physics. These phases in three dimensions arise from the topological Chern insulators in two dimensions and enjoy a degree of protection owing to the stability of Weyl points where $d_i(\boldsymbol{k}) = 0$. The Weyl points are those at which all components of $\boldsymbol{d}$ vanish, each such equation describing a surface embedded in three dimensions. Three such surfaces generically intersect at isolated points, leading to the stability of Weyl points to small perturbations

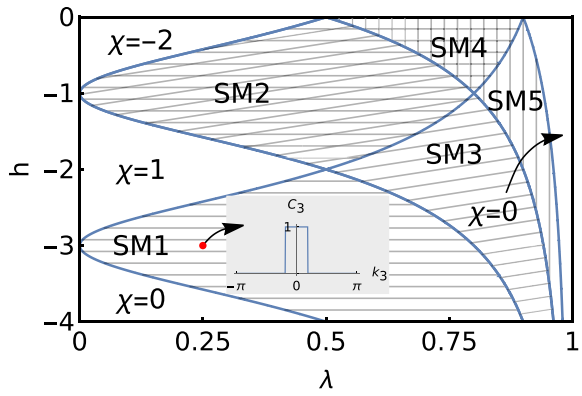

FIG. 1. Phase diagram of system in Eq. (7). Semimetallic regions with horizontal lines have band touchings at $(0, 0, \pm k_t^{(1)})$, those with vertical lines have touchings at $(\pi, \pi, \pm k_t^{(-1)})$, and those with slanted lines have touchings at $(\pi, 0, \pm k_t^{(0)})$, $(0, \pi, \pm k_t^{(0)})$, where $k_t^l = \arccos\left([\frac{\lambda}{1-\lambda} - 1 - (h+2l)^2]/[2(h+2l)]\right)$. Inset shows Chern number of T^2 submanifold of T^3 BZ labeled by k_3 for $h = -3$, $\lambda = 1/4$.

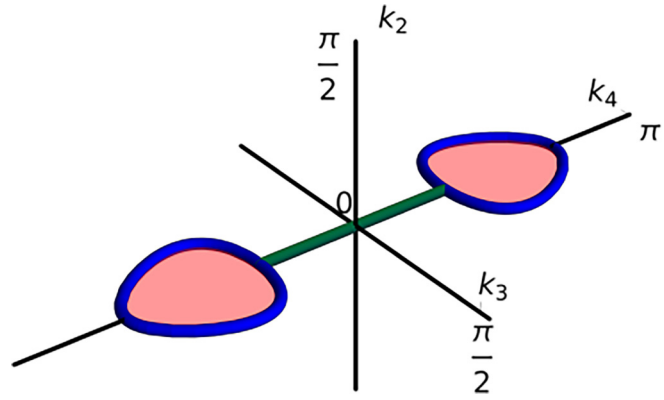

FIG. 2. Nodal line semimetal for $\lambda = 1/4$ in Eq. (8). Blue: nodal lines (nodal lines lie in the $k_1 = 0$ submanifold of T^4). The figure also depicts T^3 the *surface BZ* of the (1,0,0,0) surface. Green: Fermi arc surface states that correspond to the (1,0,0) surface states of the $\chi = 1$ Hopf insulator. Red: Drumhead surface states that correspond to the edge states of the $C_3 = 1$ Chern insulator.

of the Hamiltonian. Taking this idea to a four-dimensional two-band system, semimetallicity will require that $d_i(\boldsymbol{K}) = 0$ for $i = 1, 2, 3$ where the gap closes; $\boldsymbol{K}$ is a point in the BZ T^4 (four-torus, $[-\pi, \pi]^4$) of the 4D cubic lattice with $\boldsymbol{K} = (k_1, k_2, k_3, k_4) \equiv (\boldsymbol{k}, k_4)$. This condition, if satisfied, will be generically met on a one-dimensional submanifold of T^4. The conclusion is that the semimetals arising in these four-dimensional systems will generically possess *nodal lines*. The exciting aspect here is that these line nodes enjoy a degree of protection in that small perturbations cannot remove them but, at best, can only change their shape.

To construct such a semimetal arising from the topology of the Hopf insulator, we first study a quantum phase transition that occurs in the 3D Hopf insulator. Consider a three-dimensional system with a tuning parameter λ:

$$\boldsymbol{d}(\boldsymbol{k}, h, \lambda) = (1-\lambda)\boldsymbol{d}^{(1,1)}(\boldsymbol{k}, h) + \lambda \boldsymbol{d}^{\mathrm{f}}(\boldsymbol{k}) \tag{7}$$

where $\boldsymbol{d}^{(1,1)}(\boldsymbol{k})$ is the $\boldsymbol{d}$-vector in Eq. (3), and $\boldsymbol{d}^{\mathrm{f}}(\boldsymbol{k}) = (0, 0, 1)$ is the $\boldsymbol{d}$-vector of a gapped flat-band system which is topologically trivial. When $\lambda = 0$, the system hosts Hopf insulating phases in a regime of the parameter h, and a topologically trivial phase for $\lambda = 1$. The quantum critical point at $\lambda = 0$ that changes from $\chi = 0$ to $\chi = 1$ occurs at $h = -3$ where the two bands touch quadratically at $\boldsymbol{k} = 0$ (to be contrasted with similar touchings in dipolar Weyl semimetals [48] that does not change χ, or other systems with quadratic touchings [49]). For intermediate values of λ we obtain a variety of semimetallic phases (see Fig. 1). These semimetallic phases are characterized by a change in Chern numbers of the T^2 submanifolds of T^3 (see Ref. [43], Sec. S2), as illustrated for $\lambda = 1/4$ in Fig. 1 (inset).

We construct a semimetallic phase on a four-dimensional cubic lattice by defining for each $\boldsymbol{K} \in T^4$

$$\boldsymbol{d}(\boldsymbol{K}, \lambda) = (1-\lambda)\boldsymbol{d}^{(1,1)}(\boldsymbol{k}, -3 + \cos k_4) + \lambda \boldsymbol{d}^{\mathrm{f}}(\boldsymbol{k}). \tag{8}$$

The Hamiltonian Eq. (1) obtained using this produces a semimetallic phase for a range $0 \leqslant \lambda < 1/2$. Focusing first on $\lambda = 0$, we find that the bulk gap closes at *two points* in T^4, namely, $\boldsymbol{K}_H^{\pm}(0, 0, 0, \pm\pi/2)$, where the bands touch quadratically (see Ref. [43], Sec. S3). Most interestingly, these points are a source of "Hopf flux" in T^4; this is most easily seen by enclosing, for example, the point $\boldsymbol{K}_H^{+}$ by a ball $B^+ = |\boldsymbol{K} - \boldsymbol{K}_H^{+}| \leqslant \epsilon$, where ϵ is a small number, the boundary of this ball ∂B^+ is homeomorphic to S^3, and $\boldsymbol{d}(\boldsymbol{K}, 0)$, $\boldsymbol{K} \in \partial B^+$ defines a map from S^3 to S^2. Interestingly, the map carries a nonvanishing index $\chi = -1$, where χ is evaluated over the three-dimensional manifold ∂B^+ using the formula Eq. (4)! (see Ref. [43], Sec. S3), pointing to the topological nature of this semimetal similar to what is found in a three-dimensional Weyl semimetal.

However, as noted in the discussion above, point touching of two bands in four dimensions is not stable (in contrast with the 3D Weyl semimetal), and this is indeed seen in our construction. For a small $\lambda > 0$, we find that the two Hopf points evolve to nodal lines where the bands touch linearly except at two points on the nodal line (see Ref. [43], Sec. S3). With increasing λ, the size of the nodal lines centered around $\boldsymbol{K}_H^{\pm}$ increases. Figure 2 (thick blue lines) shows the nodal lines for $\lambda = 1/4$ in the $k_1 = 0$ T^3 submanifold of the T^4 BZ. The nodal lines appear in the k_3-k_4 plane ($k_1 = k_2 = 0$), and encircle the Hopf points $\boldsymbol{K}_H^{\pm}$ extending from $k_4^{\min} \leqslant |k_4| \leqslant k_4^{\max}$, $k_4^{\min} = \arccos\sqrt{\lambda/(1-\lambda)}$, $k_4^{\max} = \pi - \arccos\sqrt{\lambda/(1-\lambda)}$ and described by the equation

$$2(1-\cos k_3)(1-\cos k_4) + \cos^2 k_4 = \frac{\lambda}{1-\lambda}. \tag{9}$$

The nodal lines $L^{\pm}$, respectively, encircle $\boldsymbol{K}_H^{\pm}$. The intriguing aspect is that the nodal lines also carry the same Hopf number, i.e., if we place balls $B^{\pm}$ centered around $\boldsymbol{K}_H^{\pm}$, and *enclosing* the nodal lines $L^{\pm}$, then the Hamiltonian on the surface of the ball $\partial B^{\pm}$ defines a Hopf map such that the Hopf invariant associated with the $L^{\pm}$ nodal lines are opposite of each other. This demonstrates the topological origin of the nodal lines and

their stability. The nodal lines which appear between $\pm k_4^{\min}$ and $\pm k_4^{\max}$ separate three-dimensional T^3 submanifolds of T^4 that carry distinct invariants χ. Indeed, for all the T^3 submanifolds with $|k_4| < k_4^{\min}$, the invariant $\chi = 1$. This change of topology of the bands along k_4 is encoded in the Hopf number on the surface of $\partial B^{\pm}$(see Ref. [43], Sec. S3).

It can also be shown (see Ref. [43], Sec. S3) that these features found above do not arise from a linear point-group symmetry (quadratic touching of bands requires additional symmetries [50]) like crystal rotations, etc. As detailed in Ref. [43] (Sec. S3), the nodal lines are stable to such symmetry-breaking terms. Furthermore, it is shown that the specific nature of $\boldsymbol{d}^f$ (so long as it is gapped and trivial) is also not important. In fact, the semimetal is stable to any perturbation that has a $\mathcal{C}'$ symmetry, which is the composition of charge conjugation and spatial inversion [28].

We next investigate the nature of the surface states of the four-dimensional semimetal. The surface of this system is characterized by a normal direction and is a "three-dimensional crystal" with a T^3 surface Brillouin zone. Depicted in Fig. 2 for the surface with the (1,0,0,0) normal are a remarkably rich set of surface states. First, there is a set of gapless "Fermi-arc" states that exist between $\pm k_4^{\min}$, depicted by the solid green line in Fig. 2. These arise from the (1,0,0) surface states of the $\chi = 1$ Hopf insulator realized in the T^3 submanifolds in this regime of k_4. There are additional surface states that arise in the regime $k_4^{\min} < |k_4| < k_4^{\max}$. In fact, all the points in the T^3 surface BZ that are inside the nodal line projected onto the surface BZ host gapless states that are higher-dimensional analogs of drumhead states (see Ref. [33] and references therein). Details of all of these states may be found in Ref. [43], Sec. S4.

The semimetal holds further interesting aspects when we study the surface states on the (0,0,1,0) surface. This surface hosts two types of gapless states (see Fig. 3). We find first a "Fermi surface" of gapless states between $|k_4| < k_4^{\min}$; these are the surface states of the $\chi = 1$ Hopf insulator that is realized in the T^3 submanifolds. In addition, there are other gapless states shown by the blue lines of the same figure; these are gapless states corresponding to the projection of the gapless nodal line onto the surface BZ.

Finally, we also point out the possibility of interesting "corner states" in this semimetal that arise in the two-dimensional intersection of two three-dimensional surfaces. As an example, The corner formed by the intersection of two surfaces (1,0,0,0) and (0,1,0,0) will have a two-dimensional T^2 Brillouin zone labeled by (k_3, k_4). The corner states arise because the corner terminates 1-2 planes of the four-dimensional crystal. In the instance of $\lambda = 1/4$, some of the 1-2 submanifolds (which are T^2) host nonzero Chern numbers in the regime $k_4^{\min} < |k_4| < k_4^{\max}$ and should result in the "corner drumhead states" in the T^2 Brillouin zone. Other corners (intersections of different three-dimensional surfaces) will host Fermi arc states. While our calculations are consistent with this possibility, a full demonstration of this requires very large system sizes. Protected gapless phases can also be constructed from Hopf-Chern insulators, as demonstrated in Ref. [43] (see Sec. S5).

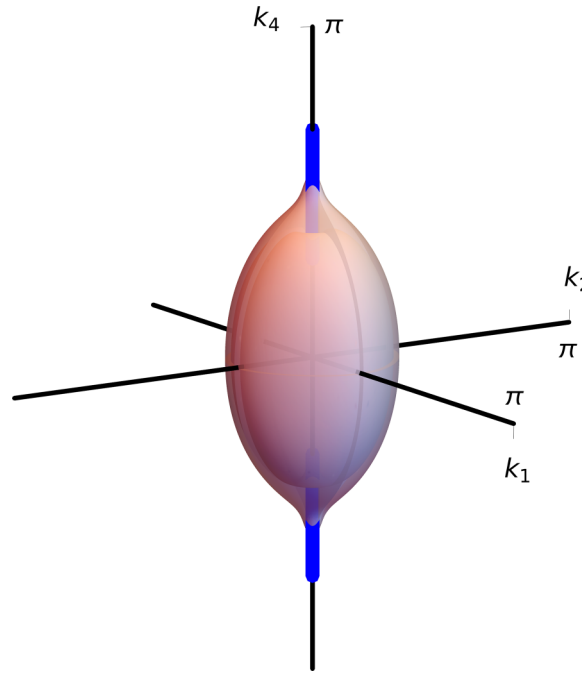

FIG. 3. Surface states of the nodal line semimetal in the (0,0,1,0) surface BZ. Red: "Fermi surface" states that correspond to the (0,0,1) surface states of the $\chi = 1$ Hopf insulator. Blue: Fermi arc states that arise from the projection of the nodal lines onto the surface BZ.

IV. THREE-DIMENSIONAL SEMIMETALS

We now turn to the construction of semimetallic phases in three dimensions protected by unstable homotopies. The class AIII in two spatial dimensions does not host any strong topological phases [8]. However, when there are two bands, the insulating phases are described by the homotopy classes of maps from T^2 (BZ in two dimensions) to S^1. Consider the Hamiltonian in Eq. (1) defined for (k_1, k_2) in the two-dimensional BZ as

$$d_1^{(n_1,n_2)}(k_1,k_2) = -t_1(\cos k_1 + \cos k_2) - t_2 \cos(n_1 k_1 + n_2 k_2),$$
$$d_2^{(n_1,n_2)}(k_1,k_2) = t_1(\sin k_1 + \sin k_2) + t_2 \sin(n_1 k_1 + n_2 k_2). \tag{10}$$

When $|t_2| > 2|t_1|$, we obtain a gapped phase with a filled valence band (at a filling of one particle per site). The insulating phase is topologically nontrivial and is characterized by nonzero winding numbers (n_1, n_2) which describe the homotopy of maps from T^2 to S^1.

We now construct semimetals in three dimensions, which are protected by the homotopies of maps from T^2 to S^1. To this end consider a Hamiltonian defined on a three-dimensional BZ:

$$d_\alpha(k_1,k_2,k_3) = \frac{1+\cos k_3}{2} d_\alpha^{(1,1)}(k_1,k_2) + \frac{1-\cos k_3}{2} d_\alpha^{(2,2)}(k_1,k_2). \tag{11}$$

This system hosts a set of nodal lines (see Fig. 4) that arise from the change of topology of the two-dimensional T^2

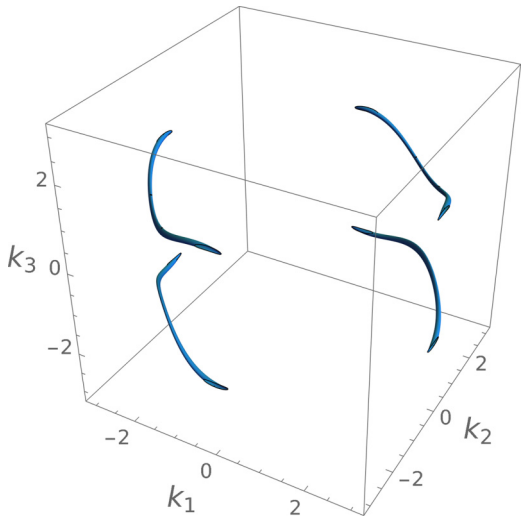

FIG. 4. Nodal lines of the three-dimensional semimetal in class AIII constructed using Eqs. (10) and (11) with $t_1 = 1, t_2 = -3$.

submanifolds of T^3 with k_3. This semimetal is to be contrasted with nodal line semimetals derived from a generalized Hopf map obtained in Ref. [51] without AIII symmetry. Our 3D semimetal also hosts interesting gapless surface states. For surfaces, with normal (1,0,0) and (0,1,0) there is a region in the two-dimensional surface BZ that hosts gapless drumhead states.

V. CONCLUDING REMARKS

The examples constructed above demonstrate the idea of creating semimetals in different dimensions that are protected by unstable homotopies. We have chosen to call these "delicate semimetals," taking inspiration from the canonical example of an unstable homotopy of maps from T^3 to S^2 that leads to Hopf insulators with delicate topology. Exploring the possibilities of experimental realization of the semimetals provides an interesting research direction. The four-dimensional delicate semimetals and their surface states may be explored by exploiting the ideas of synthetic dimensions [52] in cold atoms [53], photonic systems [54], and topoelectric circuits [29], while the AIII semimetal in two dimensions may also be realized in cold atomic systems using suitably designed optical potentials, and also topoelectric circuits.

From a theoretical perspective, it will be interesting to find generalizations of such semimetals using other recently proposed topological phases [55] in three dimensions, including generalizations to variants with a larger number of bands [28,34]. Understanding the responses [46,56], including the effects of disorder, of these delicate semimetals, also provides an exciting direction.

ACKNOWLEDGMENTS

B.P.P. thanks the PMRF program for support. V.B.S. acknowledges DST-SERB, India, for support.

[1] L. Fu, C. L. Kane, and E. J. Mele, Phys. Rev. Lett. **98**, 106803 (2007).
[2] C. L. Kane and E. J. Mele, Phys. Rev. Lett. **95**, 146802 (2005).
[3] J. E. Moore and L. Balents, Phys. Rev. B **75**, 121306(R) (2007).
[4] R. Roy, Phys. Rev. B **79**, 195322 (2009).
[5] A. Kitaev, AIP Conf. Proc. **1134**, 22 (2009).
[6] S. Ryu, A. P. Schnyder, A. Furusaki, and A. W. W. Ludwig, New J. Phys. **12**, 065010 (2010).
[7] X.-L. Qi and S.-C. Zhang, Rev. Mod. Phys. **83**, 1057 (2011).
[8] C.-K. Chiu, J. C. Y. Teo, A. P. Schnyder, and S. Ryu, Rev. Mod. Phys. **88**, 035005 (2016).
[9] R.-J. Slager, A. Mesaros, V. Juričić, and J. Zaanen, Nat. Phys. **9**, 98 (2013).
[10] W. A. Benalcazar, T. Li, and T. L. Hughes, Phys. Rev. B **99**, 245151 (2019).
[11] B. Bradlyn, L. Elcoro, J. Cano, M. G. Vergniory, Z. Wang, C. Felser, M. I. Aroyo, and B. A. Bernevig, Nature (London) **547**, 298 (2017).
[12] A. Altland and M. R. Zirnbauer, Phys. Rev. B **55**, 1142 (1997).
[13] M. R. Zirnbauer, arXiv:1001.0722.
[14] A. Agarwala, A. Haldar, and V. B. Shenoy, Ann. Phys. (NY) **385**, 469 (2017).
[15] A. H. Castro Neto, F. Guinea, N. M. R. Peres, K. S. Novoselov, and A. K. Geim, Rev. Mod. Phys. **81**, 109 (2009).
[16] A. A. Burkov, M. D. Hook, and L. Balents, Phys. Rev. B **84**, 235126 (2011).
[17] P. Hosur and X. Qi, C. R. Phys. **14**, 857 (2013).
[18] O. Vafek and A. Vishwanath, Annu. Rev. Condens. Matter Phys. **5**, 83 (2014).
[19] C. Fang, Y. Chen, H.-Y. Kee, and L. Fu, Phys. Rev. B **92**, 081201(R) (2015).
[20] B. Yan and C. Felser, Annu. Rev. Condens. Matter Phys. **8**, 337 (2017).
[21] N. P. Armitage, E. J. Mele, and A. Vishwanath, Rev. Mod. Phys. **90**, 015001 (2018).
[22] A. Burkov, Annu. Rev. Condens. Matter Phys. **9**, 359 (2018).
[23] R. Kennedy, Ph.D. thesis, University of Cologne, 2014.
[24] Homotopies of spheres, $\pi_{n+k}(S^n)$ are termed "stable" if $n > k+1$ and "unstable" if $n \leqslant k+1$. The origin of this terminology arises from the fact that the homotopy group becomes "stable," i.e., independent of n. For example, $\pi_{4+1}(S^4) = \mathbb{Z}_2$ and so is $\pi_{n+1}(S^n)$ for any $n \geqslant 3$. However, when $n = 2$, $\pi_{2+1}(S^2) = \mathbb{Z}$ (characterized by the Hopf map) is a different group from $\mathbb{Z}_2$, in this sense in "unstable" i.e., does not follow a set pattern. Indeed, such unstable homotopies are obtained when n is small compared with k, this is the sense of being "small dimensional."
[25] J. E. Moore, Y. Ran, and X.-G. Wen, Phys. Rev. Lett. **101**, 186805 (2008).
[26] D.-L. Deng, S.-T. Wang, C. Shen, and L.-M. Duan, Phys. Rev. B **88**, 201105(R) (2013).
[27] R. Kennedy, Phys. Rev. B **94**, 035137 (2016).
[28] C. Liu, F. Vafa, and C. Xu, Phys. Rev. B **95**, 161116(R) (2017).
[29] Z. Wang, X.-T. Zeng, Y. Biao, Z. Yan, and R. Yu, Phys. Rev. Lett. **130**, 057201 (2023).

[30] H. C. Po, H. Watanabe, and A. Vishwanath, Phys. Rev. Lett. **121**, 126402 (2018).
[31] A. Nelson, T. Neupert, T. Bzdušek, and A. Alexandradinata, Phys. Rev. Lett. **126**, 216404 (2021).
[32] A. Nelson, T. Neupert, A. Alexandradinata, and T. Bzdušek, Phys. Rev. B **106**, 075124 (2022).
[33] G. Bian, T.-R. Chang, H. Zheng, S. Velury, S.-Y. Xu, T. Neupert, C.-K. Chiu, S.-M. Huang, D. S. Sanchez, I. Belopolski, N. Alidoust, P.-J. Chen, G. Chang, A. Bansil, H.-T. Jeng, H. Lin, and M. Z. Hasan, Phys. Rev. B **93**, 121113(R) (2016).
[34] B. Lapierre, T. Neupert, and L. Trifunovic, Phys. Rev. Res. **3**, 033045 (2021).
[35] H. M. Price, O. Zilberberg, T. Ozawa, I. Carusotto, and N. Goldman, Phys. Rev. Lett. **115**, 195303 (2015).
[36] B. Lian and S.-C. Zhang, Phys. Rev. B **94**, 041105(R) (2016).
[37] I. Petrides, H. M. Price, and O. Zilberberg, Phys. Rev. B **98**, 125431 (2018).
[38] L. Pontrjagin, Rec. Math. [Mat. Sbornik] N.S., **9**, 331 (1941).
[39] D. Auckly and L. Kapitanski, Commun. Math. Phys. **256**, 611 (2005).
[40] D. DeTurck, H. Gluck, R. Komendarczyk, P. Melvin, C. Shonkwiler, and D. S. Vela-Vick, J. Math. Phys. **54**, 013515 (2013).
[41] M. Kobayashi and M. Nitta, Nucl. Phys. B **876**, 605 (2013).
[42] F. N. Ünal, A. Eckardt, and R.-J. Slager, Phys. Rev. Res. **1**, 022003(R) (2019).
[43] See Supplemental Material at http://link.aps.org/supplemental/10.1103/PhysRevB.109.155131 for the definition of the topological index, details concerning phase transitions in Hopf insulators and construction of delicate semimetals, a demonstration of quantization of Hopf flux, a discussion of the effect of symmetry breaking terms, details of the surface state calculations, and a discussion of delicate semimetals constructed from Hopf-Chern insulators is also included.
[44] R. Bott and L. W. Tu, *Differential Forms in Algebraic Topology* (Springer, New York, 1982).
[45] F. Wilczek and A. Zee, Phys. Rev. Lett. **51**, 2250 (1983).
[46] Y. Wang, A. C. Tyner, and P. Goswami, arXiv:2301.08244.
[47] I. Dutta and K. Saha, arXiv:2305.09616.
[48] A. C. Tyner and S. Sur, Phys. Rev. B **109**, L081101 (2024).
[49] A. Graf and F. Piéchon, Phys. Rev. B **108**, 115105 (2023).
[50] C. Fang, M. J. Gilbert, X. Dai, and B. A. Bernevig, Phys. Rev. Lett. **108**, 266802 (2012).
[51] M. Ezawa, Phys. Rev. B **96**, 041202(R) (2017).
[52] T. Ozawa and H. M. Price, Nat. Rev. Phys. **1**, 349 (2019).
[53] M. Lohse, C. Schweizer, H. M. Price, O. Zilberberg, and I. Bloch, Nature (London) **553**, 55 (2018).
[54] O. Zilberberg, S. Huang, J. Guglielmon, M. Wang, K. P. Chen, Y. E. Kraus, and M. C. Rechtsman, Nature (London) **553**, 59 (2018).
[55] Z. Davoyan, W. J. Jankowski, A. Bouhon, and R.-J. Slager, arXiv:2308.15555.
[56] A. Sekine and K. Nomura, J. Appl. Phys. **129**, 141101 (2021).